Solutions of laminar mud flow on rectangular channel

Ko-Fei Liu (*Dept. of Civil Engineering, National Taiwan University, Taiwan R.O.C*)
Shih-Chao Wei (*Dept. of Civil Engineering, National Taiwan University, Taiwan R.O.C*)

Abstract Mudflow is a common phenomenon in mountainous area. A lot of researches had simulated debris flows with mudflow. However, either numerical analysis or approximate solutions needs a fundamental solution to work with. In the present paper, we focused on the analytical solutions of fluid mud by using the Bingham fluid model. By using the fact that boundary layer is thin, the solutions of steady uniform flow can be constructed on an inclined rectangular channel. The results can be expressed as function of depth ratio between shear layer to whole layer and Bingham number. The limiting cases for narrow channel and wide one can be discussed by changing the depth width ratio. The solutions on wide channel are the same as other research.
Keywords Mud Flows, Bingham fluid model, Steady Uniform Flow.

1. Introduction

Mud flows is one of several forms of debris flows, and it can be triggered by landslide, torrential rains, or volcanic eruptions. The characteristic feature is plastic-like behavior, and the shear stress must exceed the yield stress to drive the fluid flowing. Some analytical solutions with a yield stress had been studied. Liu and Mei (1989) had provided theories for slow flow in a thin layer on an inclined plane. Balmforth and Craster (1999) had discussed the lubrication theory for fluid flowing down an inclined plane. Mei and Yuhi (2001) extended the approximate theory of Liu & Mei (1989) from two to three dimensions for a thin layer of Bingham fluid flowing down an open channel of finite width. But there is no analytical solution given for a steady uniform flow in finite width rectangular channel.

2. Formulation

2.1 Long Wave Approximation

We consider a three-dimensional laminar flow of mud flowing down a rectangular channel inclined at the angle θ with respect to the horizontal. In the standard rectangular channel as shown in Fig. 1 (a), the order of width and depth are the same. The x-axis coincides with longitudinal axis along the channel bottom. The y-axis is in the transverse direction and the z-axis is perpendicular to both the x- and y-axis as shown in Fig. 1(a). The governing equations are the continuity equation and momentum conservation equations. Following long-wave expansions, the equations of motion are approximated as follows:

$$\frac{\partial u}{\partial x}+\frac{\partial v}{\partial y}+\frac{\partial w}{\partial z}=0\,, \tag{1}$$

$$\left(\frac{\partial u}{\partial t}+u\frac{\partial u}{\partial x}+v\frac{\partial u}{\partial y}+w\frac{\partial u}{\partial z}\right)=-\frac{1}{\rho}\frac{\partial p}{\partial x}+g\sin\theta+\frac{1}{\rho}\left(\frac{\partial \tau_{yx}}{\partial y}+\frac{\partial \tau_{zx}}{\partial z}\right), \tag{2}$$

$$0=\frac{1}{\rho}\frac{\partial p}{\partial y}, \tag{3}$$

$$0=\frac{1}{\rho}\frac{\partial p}{\partial z}+g\cos\theta\,, \tag{4}$$

where u, v, w are velocity components in x, y, z directions, and p is the pressure, t is the time, ρ is the fluid density, g is the gravitational acceleration. With zero pressure at the free surface, the pressure at a distance z above the bed is obtained from (4) as

$$p = \rho g(h - z)\cos\theta \,. \tag{5}$$

Substituting Eq. (5) into Eq. (3), we can obtain $\partial h / \partial y = 0$. This relation implies the flow depth does not vary in y-direction. Considering steady uniform flow in x direction, with $\partial u / \partial x = 0$, continuity eq. becomes

$$\frac{\partial v}{\partial y} + \frac{\partial w}{\partial z} = 0 \,. \tag{6}$$

Substituting Eq. (5) into Eq. (2), the momentum equation can be reduced to

$$\left(v\frac{\partial u}{\partial y} + w\frac{\partial u}{\partial z} \right) = g\sin\theta + \frac{1}{\rho}\left(\frac{\partial \tau_{yx}}{\partial y} + \frac{\partial \tau_{zx}}{\partial z} \right), \tag{7}$$

because flow depth remains the same for uniform flow. In this work, constitutive law of Bingham fluid is used to approximate muddy flows as follows

$$E = 0 \ , \quad \tau \le \tau_0 \,, \tag{8}$$

$$\tau_{ij} = (\frac{\tau_0}{E} + \mu)E_{ij} \quad , \quad \tau > \tau_0 \,, \tag{9}$$

where

$$E = (\frac{1}{2}E_{ij}E_{ij})^{\frac{1}{2}} \ \text{,and} \ \ \tau = (\frac{1}{2}\tau_{ij}\tau_{ij})^{\frac{1}{2}}; \tag{10}$$

where E_{ij} and τ_{ij} are the rate-of-strain tensor and stress tensor respectively, τ_0 is the yield stress, and μ is the dynamic viscosity. Because of the constitutive relation, the flow can be separated by yield stress as shown in Fig. 1(b), (c). In general, one can regard the $\tau > \tau_0$ region as shear layer and regard the $\tau < \tau_0$ region as plug layer where there is no strain rate in site according for Eq. (8).

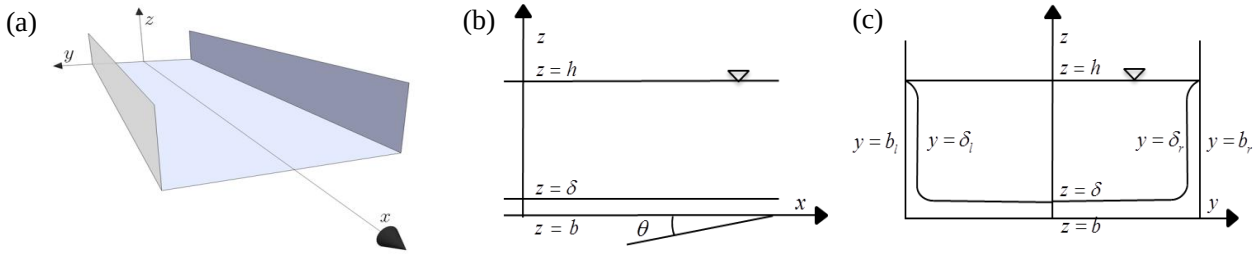

Fig. 1 (a) Standard Rectangular Channel, (b) $x - z$ direction profile, (c) $y - z$ direction profile.

In Fig. 1(b), (c), $z = b$ is the bed, $y = b_l$, $y = b_r$ are the side banks, and no-slip condition is used along all solid boundary. $z = \delta$ indicates the yield surface (the interface between shear layer and plug layer) near bed, and $y = \delta_l, y = \delta_r$ are also the yield surface near the side banks. On the yield surface, all values must be continuous. From the constitutive law, the strain rate is equal to 0 at the yield surface $z = \delta, y = \delta_l, y = \delta_r$, so

$$E = \left[\left(\frac{\partial u}{\partial y} \right)^2 + \left(\frac{\partial u}{\partial z} \right)^2 \right]^{1/2} = 0 \text{, as } \ \delta_l \le y \le \delta_r, \ \ \delta \le z \le h \,. \tag{11}$$

At the free surface $z = h$, there are the kinematic boundary condition (KBC)

$$w = v\frac{\partial h}{\partial y} \quad \text{at} \quad z = h\,, \tag{12}$$

and dynamic boundary condition (DBC)

$$\tau_{zx} = 0 \quad \text{at} \quad z = h\,. \tag{13}$$

2.2 Thin Shear Layer Approximation

In order to understand the relation between the shear layer's thickness and flow depth, we use the following scales for the problem

$$x = O(L),\ \ y = O(D),\ \ z = O(H),\ \ y_\delta = O(D_\delta),\ \ z_\delta = O(H_\delta), \tag{14}$$

where the subscript δ means in the shear layer. From Table 1, one can estimate the scale L to be $O(100m)$, D to be $O(10m)$ by gully width, and H to be $O(10m)$.

Table 1. Characteristics of debris flow caused by Typhoon Herb (1996) in the Chenyoulan stream watershed, Taiwan. (Data from Jan and Chen, 2005)

Location	Debris flow type	Gully width (m)	Alluvial Fan			Gully slope		
			Max. length (m)	Max. width (m)	Average depth (m)	Initiation (degree)	Transportation (degree)	Deposition (degree)
Junkengkou	Bouldery	5	310	95	4	33.7	16.0	16.0
Junkengqiao	Cobble-gravely	5	228	130	4	25.2	12.0	9.1
Xinyizhongxin	Cobble-gravely	4	95	60	3	23.1	18.0	6.0
Sangfengqiu	Cobble-gravely	5	76	95	3	34.6	16.0	7.0
Fengqiu	Bouldery	9	400	570	5	27.4	18.0	5.7
Tongfu	Muddy	6	95	230	3	27.2	17.8	8.5
Longhua	Muddy	6	250	190	4	28.6	15.0	15.0
Shenmu	Cobble-gravely	12	800	90	4	29.3	11.2	7.4

The scale of velocity in x-direction is $O(U)$ and Eq.(1) provides the scale for the other velocity component as

$$u = O(U),\ \ v = O(\frac{UD}{L}),\ \ z = O(\frac{UH}{L}) \tag{15}$$

In Liu and Lai (2000), the shear layer's thickness in z-direction can be estimated by the balance of bottom pressure gradient and shear stress in the x-momentum equation of shear layer as

$$H_\delta = \sqrt{\frac{\mu U}{\rho g \cos\theta}\frac{L}{H}}\,, \tag{16}$$

In the field, a typical length scale $L = 100m$, depth scale $H = 10m$, velocity scale $U = 5m/s$, and $\cos\theta \approx 1$ can usually be observed. So we use the scale values and take datum in Arattano et al. (2007) into Eq. (16) as shown in Table 2, we find that the scale of thickness of shear layer is about $0.1\,m$ for low dynamic viscosity, and is about $1.5\,m$ for high dynamic viscosity. Comparing with flow depth scale ($H = 10m$), the result implies that the order of the shear layer's thickness is negligible to the leading. The thickness of side shear layer is estimated in the same way. Applying the characteristics of the thin shear layer, we can divide the flow region into three parts; plug flow region, shear layer region near bed, shear layer region near side banks as shown in Fig. 2.

Table 2. Scale estimate of thickness of shear layer. (* Data were obtained by numerical simulation.)

Torrent	Aspect	Length (m)	Width (m)	Depth (m)	μ $(Pa\cdot s)$	ρ $\left(kg/m^3\right)$	Reference	H_δ (m)	H_δ/H $(\%)$
Faucon stream	Muddy	500*	NA	10-20*	50	2000	Rema îre et al.(2005)	0.35	3.54
Anhui Dam (21.7m hight)	Mud/Debries flow	1210	210-580	NA	2.1	1600	Jin&Fread(1999)	0.08	0.81
Aberfan Dam (37m hight)	Mud/Debries flow	600*	NA	9*	958	1800	Jin&Fread(1999)	1.63	16.31
Rudd Creek (30m hight)	Mud/Debries flow	350*	30-230	0.6-3.7*	958	1600	Jin&Fread(1999)	1.73	17.30

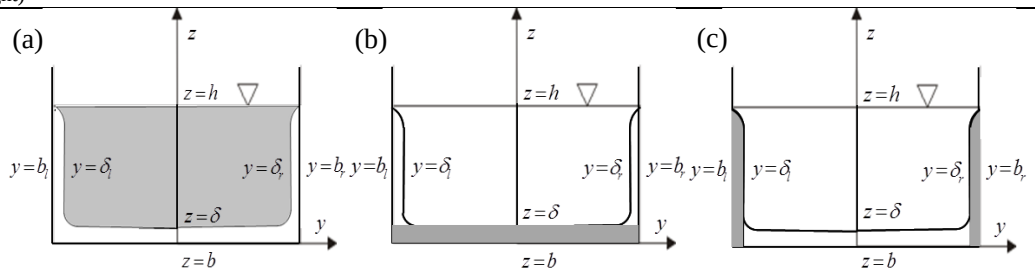

Fig. 2 (a) Plug layer region, (b) Shear layer near bed, (c) Shear layer near side bank.

2.3 Plug Layer Region

Due to thin shear layer, the governing equations can be estimated the same as Eq.(6), (7), and Eq. (12), (13) are used on free surface. In all yield surfaces, the continuation of velocity is applied, and the stress is equivalent to yield stress by constitutive law. By applying Eq. (11), Eq. (7) can be reduced to

$$0 = g\sin\theta + \frac{1}{\rho}\left(\frac{\partial \tau_{yx}}{\partial y} + \frac{\partial \tau_{zx}}{\partial z}\right). \tag{17}$$

Integrating Eq.(17) with respect to the cross section for plug region (from $z=\delta$ to $z=h$, and from $y=\delta_l$ to $y=\delta_r$), we obtain

$$0 = \rho g\sin\theta(h-\delta)(\delta_r-\delta_l) + \int_\delta^h (\tau_{yx}\big|_{\delta_r} - \tau_{yx}\big|_{\delta_l})dz + \int_{\delta_l}^{\delta_r} (\tau_{zx}\big|_h - \tau_{zx}\big|_\delta)dy\,. \tag{18}$$

Then applying Eq. (13), and $\tau_{zx}=\tau_0$ at $z=\delta$, $\tau_{yx}=\tau_0$ at $y=\delta_l$, $\tau_{yx}=-\tau_0$ at $y=\delta_r$, Eq. (21) gives

$$\frac{\tau_0}{\rho g\sin\theta} = \frac{(h-\delta)(\delta_r-\delta_l)}{2(h-\delta)+(\delta_r-\delta_l)}. \tag{19}$$

At the initiation of mud, $\delta=b$, $\delta_l=b_l$, $\delta_r=b_r$ due to the shear layers do not exist, so Eq.(19) gives

$$\tau_0 = \frac{\rho g\sin\theta(h-b)(b_r-b_l)}{2(h-b)+(b_r-b_l)}. \tag{20}$$

The above equation is the balance condition between shear stress and yield stress, and the fluid muds will start to flow as the shear stress lager than yield stress, so the starting relation can be obtained as follows

$$\frac{\rho g\sin\theta(h-b)(b_r-b_l)}{2(h-b)+(b_r-b_l)} \geq \tau_0\,, \tag{21}$$

and provide us a threshold for examining if the fluid mud is flowing or not.

2.4 Shear Layer Region near Bed

The thickness of shear layer near bed can be proved is less than depth, i.e. it is less than width as well. Therefore, the governing equation must be re-estimated by method of order magnitude. The Eq. (6), (7) can be re-estimated as

$$\frac{\partial v}{\partial y}+\frac{\partial w}{\partial z}=0\,,$$

$$\text{Scale:}\quad O(\tfrac{U}{L})\ll O(\tfrac{HU}{H_\delta L}) \tag{22}$$

$$\left(v\frac{\partial u}{\partial y}+w\frac{\partial u}{\partial z}\right)=g\sin\theta+\frac{1}{\rho}\left(\frac{\partial \tau_{yx}}{\partial y}+\frac{\partial \tau_{zx}}{\partial z}\right),$$

$$\text{Scale:}\quad O(\tfrac{U^2}{L})\ll O(\tfrac{HU^2}{H_\delta L})\qquad\qquad O(\tfrac{\mu U}{\rho D^2})\ll O(\tfrac{\mu U}{\rho H_\delta^2}) \tag{23}$$

because shear layer depth is much less than the width scale, so Eq. (22), (23) in the leading order is

$$\frac{\partial w}{\partial z}=0\,. \tag{24}$$

$$w\frac{\partial u}{\partial z}=g\sin\theta+\frac{1}{\rho}\frac{\partial \tau_{zx}}{\partial z}\,, \tag{25}$$

where the stress τ_{zx} can be expended as

$$\tau_{zx}=\mu\frac{\partial u}{\partial z}+\tau_0\,\mathrm{sgn}\left(\frac{\partial u}{\partial z}\right). \tag{26}$$

The boundary condition on the bottom is no-slip condition, and Eq. (11) in the leading order gives

$$\frac{\partial u}{\partial z}=0\,,\ \text{at}\ \ z=\delta\,. \tag{27}$$

By applying the no-slip condition on bed, Eq.(27) gives $w=0$, and Eq. (25) can be deduced

$$0=g\sin\theta+\frac{1}{\rho}\frac{\partial \tau_{zx}}{\partial z}\,, \tag{28}$$

By applying the constitutive law, we know the $\tau_{zx}=\tau_0$ at $z=\delta$, so one can integrate Eq. (28) from bed ($z=b$) to yield surface ($z=\delta$) and obtain the bottom shear stress as

$$\tau_b=\tau_0+\rho g(\delta-b)\sin\theta\,,\ \text{at}\ \ z=b\,. \tag{29}$$

Then substituting Eq. (26) to Eq. (28) gives

$$0=\rho g\sin\theta+\mu\frac{\partial^2 u}{\partial z^2}\,. \tag{30}$$

Applying Eq. (27) and no-slip condition on bed, Eq. (30) gives velocity distribution inside the bottom shear layer as

$$u=\frac{\rho g\sin\theta}{\mu}\left(\delta(z-b)-\frac{z^2-b^2}{2}\right),\ \text{as}\ \ b\le z\le\delta\,. \tag{31}$$

2.5 Shear Layer Region near Side Banks

The Eq. (6), (7) can be re-estimated the same way as in the previous section

$$\frac{\partial v}{\partial y}+\frac{\partial w}{\partial z}=0\,,$$

$$\text{Scale:}\quad O(\tfrac{DU}{D_\delta L})\gg O(\tfrac{U}{L}) \tag{32}$$

$$\left(v\frac{\partial u}{\partial y}+w\frac{\partial u}{\partial z}\right)=g\sin\theta+\frac{1}{\rho}\left(\frac{\partial \tau_{yx}}{\partial y}+\frac{\partial \tau_{zx}}{\partial z}\right),$$

$$\text{Scale:}\quad O(\tfrac{DU^2}{D_\delta L})\gg O(\tfrac{U^2}{L})\qquad\qquad O(\tfrac{\mu U}{\rho D_\delta^2})\gg O(\tfrac{\mu U}{\rho H^2}) \tag{33}$$

, ,

so Eq. (32), (33) in the leading order gives

$$\frac{\partial v}{\partial y} = 0\,, \tag{34}$$

$$v\frac{\partial u}{\partial y} = g\sin\theta + \frac{1}{\rho}\frac{\partial \tau_{yx}}{\partial y}\,, \tag{35}$$

where the stress τ_{yx} can be expended as

$$\tau_{yx} = \mu\frac{\partial u}{\partial y} + \tau_0\,\mathrm{sgn}\left(\frac{\partial u}{\partial y}\right). \tag{36}$$

The boundary conditions on side banks are no-slip condition, and Eq. (11) in the leading order gives

$$\frac{\partial u}{\partial y} = 0\,, \text{ at } \; y = \delta_l\,, y = \delta_r\,. \tag{37}$$

Using the no-slip condition on side banks, Eq. (34) gives $v = 0$, and Eq. (35) can be deduced

$$0 = \rho g\sin\theta + \frac{\partial \tau_{yx}}{\partial y}\,. \tag{38}$$

Due to the $\tau_{yx} = \tau_0$ at $y = \delta_l$ and $\tau_{yx} = -\tau_0$ at $y = \delta_r$, the shear stress on bank of left side and right side can be obtained respectively as below

$$\tau_l = \tau_0 + \rho g(\delta_l - b_l)\sin\theta\,, \text{ at } \; y = b_l\,, \tag{39}$$

$$\tau_r = -\tau_0 + \rho g(\delta_r - b_r)\sin\theta\,, \text{ at } \; y = b_r\,. \tag{40}$$

Then substituting Eq. (36) to Eq. (38) gives

$$0 = \rho g\sin\theta + \mu\frac{\partial^2 u}{\partial y^2}. \tag{41}$$

Applying Eq. (37) and no-slip condition on side banks, Eq. (41) gives velocity distribution inside the shear layer near left side and right side respectively as follows

$$u = \frac{\rho g\sin\theta}{\mu}\left(\delta_l(y - b_l) - \frac{y^2 - b_l^{\,2}}{2}\right), \text{as } \; b_l \le y \le \delta_l\,, \tag{42}$$

$$u = \frac{\rho g\sin\theta}{\mu}\left(\delta_r(y - b_r) - \frac{y^2 - b_r^{\,2}}{2}\right), \text{as } \; \delta_r \le y \le b_r\,. \tag{43}$$

3 Discussion of solutions

3.1 Rearranging the solutions

The velocity of plug layer should be a constant and the same result should be derived from Eq. (31), (42) or (43). Applying continuation of velocity on yield surface, we obtain

$$u_p = \frac{\rho g(\delta - b)^2\sin\theta}{2\mu} = \frac{\rho g(\delta_l - b_l)^2\sin\theta}{2\mu} = \frac{\rho g(\delta_r - b_r)^2\sin\theta}{2\mu}\,, \tag{44}$$

where the subscript p means plug layer. Eq. (44) gives

$$\tilde{\delta} = \left|\delta - b\right| = \left|\delta_l - b_l\right| = \left|\delta_r - b_r\right|. \tag{45}$$

So shear layer thickness is the same along all solid boundary. Substituting $\tilde{\delta}$ for all boundary layer thickness, Eq. (19) becomes

$$\frac{\tau_0}{\rho g\sin\theta} = \frac{(h - b - \tilde{\delta})(b_r - b_l - 2\tilde{\delta})}{2(h - b - \tilde{\delta}) + (b_r - b_l - 2\tilde{\delta})}\,. \tag{46}$$

Using Eq.(44), (45), velocity profiles inside the shear layers can be rewritten as

$$u = \frac{u_p}{\tilde{\delta}^2}\left[2\delta(z-b) - \left(z^2 - b^2\right)\right], \text{ as } \; b \le z \le \delta, \tag{47}$$

$$u = \frac{u_p}{\tilde{\delta}^2}\left[2\delta_l(y-b_l) - \left(y^2 - b_l^2\right)\right], \text{ as } \; b_l \le y \le \delta_l, \tag{48}$$

$$u = \frac{u_p}{\tilde{\delta}^2}\left[2\delta_r(y-b_r) - \left(y^2 - b_r^2\right)\right], \text{ as } \; \delta_r \le y \le b_r. \tag{49}$$

Likewise, the stress on bottom and side banks (Eq. (29),(39),(40)) can be rewritten as

$$\tau_b = \tau_0 + \rho g\tilde{\delta}\sin\theta, \text{ at } \; z = b, \tag{50}$$

$$\tau_l = \tau_0 + \rho g\tilde{\delta}\sin\theta, \text{ at } \; y = b_l, \tag{51}$$

$$\tau_r = -\tau_0 - \rho g\tilde{\delta}\sin\theta, \text{ at } \; y = b_r. \tag{52}$$

3.2 Important parameters

We define the non-dimensional parameters as below

$$\sigma = \frac{H}{D}, \;\; \alpha = \frac{\tau_0}{\rho g H \sin\theta}, \tag{53}$$

where σ is a depth to width ratio of the rectangular channel. α is the Bingham number, which is a measure of the yield stress relative to the horizontal pressure gradient acting over the thickness of the fluid. When α approaches zero, the fluid can be considered as Newtonian fluid. Then, Eq. (21) and (46) can be written as

$$\frac{(\frac{h}{H} - \frac{b}{H})(\frac{b_r}{D} - \frac{b_l}{D})}{2\sigma(\frac{h}{H} - \frac{b}{H}) + (\frac{b_r}{D} - \frac{b_l}{D})} > \alpha, \tag{54}$$

$$\alpha = \frac{(\frac{h}{H} - \frac{b}{H} - \frac{\tilde{\delta}}{H})(\frac{b_r}{D} - \frac{b_l}{D} - 2\frac{\tilde{\delta}}{D})}{2\sigma(\frac{h}{H} - \frac{b}{H} - \frac{\tilde{\delta}}{H}) + (\frac{b_r}{D} - \frac{b_l}{D} - 2\frac{\tilde{\delta}}{D})}. \tag{55}$$

Considering the steady uniform flow with constant depth in rectangular channel, one can let $\frac{h}{H} = 1$, $\frac{b}{H} = 0$, $\frac{b_r}{D} = 1$, $\frac{b_l}{D} = -1$, $H_\delta = D_\delta$ and substitute to the above equations to obtain

$$\frac{1}{\sigma + 1} > \alpha, \tag{56}$$

$$\frac{H_\delta}{H}\delta^* = 1 - \left(\sigma + 1\right)\alpha, \tag{57}$$

where $\delta^* = \frac{\tilde{\delta}}{H_\delta}$. By the Eq. (44), the order of velocity in x- component can be estimated as

$$U = O\left(\frac{\rho g H^2 \sin\theta}{\mu}\right). \tag{58}$$

By applying Eq. (57), (58), Eq. (44) gives

$$u_p^* = \frac{\left(1 - \left(\sigma + 1\right)\alpha\right)^2}{2}, \tag{59}$$

where $u_p^* = \frac{u_p}{U}$. In Eq. (56), (57), (59), one can shift the value of σ briefly to obtain the starting condition, thickness of shear layer, and plug layer's velocity. Some cases can be shown as the following table.

Table 3 Cases on different σ

Case	Ratio of depth to width	Starting condition	Thickness of shear layer	Velocity of plug layer
wide channel	$\sigma \ll 1$	$\alpha < 1$	$\frac{H_\delta}{H}\delta^* \cong 1-\alpha$	$u_p^* \cong \frac{(1-\alpha)^2}{2}$
stander channel	$\sigma = 1$	$\alpha < \frac{1}{2}$	$\frac{H_\delta}{H}\delta^* = 1-2\alpha$	$u_p^* = \frac{(1-2\alpha)^2}{2}$
narrow channel	$\sigma \gg 1$	$\alpha < \frac{1}{\sigma}$	$\frac{H_\delta}{H}\delta^* \cong 1-\sigma\alpha$	$u_p^* \cong \frac{(1-\sigma\alpha)^2}{2}$

In Eq. (56), one can find the starting condition is associated the channel's shape with Bingham number. If the channel is much wider, the fluid is much easier to start flowing. However, if the Bingham number α approaches zero, the fluid can be seen as Newtonian fluid. Therefore, the starting condition only can be accepted for $\alpha > 0$. In Table 3, the wide channel's solutions can be compared to Liu and Mei (1989), the thickness of shear layer and the velocity of plug layer are the same under steady uniform flow.

5 Conclusion

In this study, the Bingham constitutive law is used to model the mud flows, and we derive the solutions of steady uniform flow in an inclined rectangular channel. The velocity profile for rectangular channel with depth to width ratio of order unity is derived. The solutions on wide channel are verified to be the same as Liu and Mei (1989). The boundary shear layer thickness is found to be the same along all solid boundaries and regardless of the depth to width ratio. The mud can start to flow only if a starting condition based on Bingham number is satisfied. The solutions can provide a basis for further studies on instability problem or verification of numerical experiments.

Acknowledgments

References

Arattano, M., Franzi, L., (2007). Debris flow rheology assessment through mathematical simulation of hydrograph deformation, The Fourth International Conference on Debris-Flow Hazards Mitigation, 99-109.

Balmforth, N.J., Craster, R.V., (1999). A Consistent Thin-Layer Theory For Bingham Fluids. J. on-Newtonian Fluid Mech., 84, 65-81.

Balmforth, N. J., Mandre, J.S., (2004). Dynamics of Roll Waves. J. Fluid Mech., 514, 1-33.

Balmforth, N.J., Liu, J.J. , (2004). Roll Waves in Mud. J. Fluid Mech., 519, 33-54.

Jin, M., Fread, d. (1999). 1D Modeling of Mud/Debris Unsteady Flows. J. Hydraul. Eng., 125(8), 827-834.

Jan, C.D., Chen, C.L. (2005). Debris flows caused by Typhoon Herb in Taiwan. Debris-flow Hazards and Related Phenomena, 239-263.

Liu, K.F., Mei, C.C., (1989). Slow spreading of a sheet of Bingham fluid on an inclined plane. J. Fluid Mech., 207, 505-529.

Liu, K.F., Mei, C.C., (1994). Roll Waves on A Layer of a Muddy Fluid Flowing Down a Gentle Slope - A Bingham Model. Physics of Fluids, 6, 2577-2590.

Liu, K.F., Lai, K.W., (2000). Numerical Simulation of Two Dimensional Debris Flows. The Second International Conference on Debris-Flow Hazards Mitigation, 531-535.
Mei, C.C., Liu, K.F., Yuhi, M., (2001). Mud Flow— Slow and Fast. Lecture Notes in Physics, 582, 548-577.
Mei, C.C., Yuhi, M., (2001). Slow Flow of a Bingham Fluid In a Shallow Channel of Finite Width. J. Fluid Mech., 431, 135-159.
Ng, C-O., Mei, C.C., (1994). Roll waves on a shallow layer of mud modelled as a power-law fluid. J. Fluid Mech., 263, 151-183.
O'Brien, J., Julien, P.Y., (1988). Laboratory analysis of mudflow properties. Journal of Hydraulic Engineering, 114(8), 877-887.
Rema îre, A., Malet, J.-P., Maquaire, O., Ancey, C. and Locat, J. (2005), Flow behaviour and runout modelling of a complex debris flow in a clay-shale basin. Earth Surf. Process and Landforms, 30, 479-488.

K.F. Liu
Dept. of Civil Engineering, Hydraulic Division.
National Taiwan University, Taiwan, R.O.C.
No. 1, Sec. 4, Roosevelt Rd., 10617, Taipei, Taiwan, R.O.C.
e-mail: kfliu@ntu.edu.tw

S.C. Wei
Dept. of Civil Engineering, Hydraulic Division.
National Taiwan University, Taiwan, R.O.C.
No. 1, Sec. 4, Roosevelt Rd., 10617, Taipei, Taiwan, R.O.C.
e-mail: d01521001@ntu.edu.tw